

# Numerical Modeling of Vertical Axis Hydro Turbine with Experimental Validation

Ahmad Yasim<sup>1</sup>, Mukhtasor<sup>1</sup>, Shade Rahmawati<sup>1</sup>, Widodo<sup>2</sup> and Madi<sup>1</sup>

<sup>1</sup>Department of Ocean Engineering, Institute of Technology Sepuluh Nopember (ITS), Surabaya 60111, Indonesia

<sup>2</sup>Hydrodynamic Institute of Technology, Agency for the Assessment and Application of Technology, Surabaya, Indonesia

**Keywords:** Darrieus Turbine, CFD, Validation, Torque, Coefficient of Turbine Performance.

**Abstract:** Ocean current energy is an energy source that has great potential in Indonesia but is dominated by low current velocity. Many potential locations such as Riau, Boleng, and Mansuar strait only have the maximum current speed by 1.39 m/s, 1.5 m/s, and 1.79 m/s. Therefore, energy conversion technology is needed that is able to exploit the potential of low-speed current energy into electricity. Darrieus turbine is a type of vertical axis hydro turbine that is suitable to be developed in Indonesian waters because it can work at a lower current speed than the other types. To study the Darrieus turbine performance on a low-speed ocean current, numerical modeling based on computational fluid dynamics (CFD) which is validated with experimental results must be done. The numerical validation uses Darrieus turbine experimental data with diameter 0.91 m, chord blade 0.07 m and span 0.7 m. The validation process starts with defining boundary geometry dimension, meshing construction and turbulence model suitable. The simulation is carried out at the current speed of 1.5 m/s with TSR variations. The validation parameter is the torque value that correlates with the coefficient of turbine performance. As the result obtained validation rate with the average error of 7.3%.

## 1 INTRODUCTION

Ocean current energy is one of the marine energy sources that has great potential in Indonesia. Ocean currents are the movements of a mass of water caused by winds, density differences, tidal activity or long-wave movements (Daruwedho, 2016). The potential of ocean current energy in Indonesia is dominated by low current velocity. Some potential locations such as the Riau Strait, Boleng Strait, and Mansuar Strait only have a maximum current velocity of 1.39 m/s, 1.5 m/s, and 1.79 m/s (Mukhtasor, et. al., 2014). This figure is smaller than the current velocity at the location of the Sea Gen turbine placed, Northern Ireland, which is 2.5 m/s or at the location of the largest tidal current turbine namely Scotrenewables SR2000, Orkney, UK, where the current velocity is 3 m/s (MeyGen, 2019). Because Indonesia has a relatively low current velocity, research that focused on developing low-speed current turbines is important.

Darrieus turbine is a type of vertical axial tidal current turbine (VATCT) that is suitable to be developed in Indonesian waters because it is able to extract ocean currents from various directions and

works at lower current speeds compared to other turbine types (Hantoro, et.al., 2009, 2011, 2018; Rachmat, 2015; Kasharjanto, et.al., 2017). To do more advanced research about Darrieus turbine performance, numerical modeling based on computational fluid dynamics (CFD) was conducted.

CFD is a numerical program developed to quantitatively analyze fluid flow, heat transfer, pressure, energy, and chemical reactions. There are several procedures to do a simulation in CFD, such as creating a geometry model, mesh generation, definite solver, checking results, and presenting numerical output. The use of CFD methods in research must pass the validation process to ensure the numerical output are correct. According to Marsh, et. al. (2015), the validation process of the Darrieus turbine numerical modeling includes studies of boundary condition size, number of grids, and definite solver. Good numerical modeling is validated with experimental results. Therefore, this study will focus on numerical modeling procedures to obtain validated results with experimental results.

However, the use of a 3D model in a simulation requires a supercomputer facility and takes a long time for running simulation (Marsh, et. al., 2015).

According to Dai, et. al. (2009), shaft and strut parts are not needed to include in a numerical simulation of Darrieus turbine if only for analyzing a hydrodynamics performance. Without strut, the numerical modeling of a Darrieus turbine can be converted from a 3D model to a 2D model, so that with the 2D model, the simulation would become lighter and faster.

## 2 COMPUTATIONAL FLUID DYNAMICS OF TURBINE

### 2.1 RANS Governing Equations

The average motion equation for fluid flow is generally better known as Reynolds Averaged Navier-Stokes Equation. The RANS equation uses a turbulent model to model all large and small scale motion based on the average quantity of flow or model approach. The modeling approach results in a loss of all spectral effects in the time averaging process (Mulualem, 2003).

The unsteady RANS modeling approach solves the Reynolds averaged equations of mass and momentum conservation given in equation 1 and equation 2.

$$\frac{\partial \bar{U}_i}{\partial x_i} = 0 \quad (1)$$

$$\begin{aligned} \frac{\partial \bar{U}_i}{\partial t} + \frac{\partial}{\partial x_j} (\bar{U}_i \bar{U}_j) = & -\frac{1}{\rho} \int \left( \frac{\partial \bar{p}}{\partial x_i} + \delta_{i1} \frac{\partial (P)}{\partial x_1} \right) \\ & + \frac{\partial}{\partial x_j} \left( v \frac{\partial \bar{U}_i}{\partial x_j} - \bar{U}_i' U_j' \right) \\ & + \rho g_i + \bar{F}_s + \bar{F}_b \end{aligned} \quad (2)$$

where the bar  $(\bar{\cdot})$  defines the time averaged components;  $\bar{U}$  adalah is the Reynolds averaged velocity;  $\bar{p}$  is the Reynolds averaged pressure;  $v$  is a kinematic viscosity;  $\delta_{i1}$  is the Kronecker-delta,  $\frac{\partial (P)}{\partial x_1}$  is driving force, a constant streamwise pressure gradient, and  $\bar{U}_i' U_j'$  are the Reynolds stresses. The Reynolds stresses are defined as.

$$\bar{U}_i' U_j' = v \left( \frac{\partial \bar{U}_i}{\partial x_j} - \frac{\partial \bar{U}_j}{\partial x_i} \right) - \frac{2}{3} k \delta_{ij} \quad (3)$$

Turbulent kinetic energy and dissipation rate can be definite using equation 4 and equation 5.

Turbulent kinetic energy:

$$\frac{\partial k}{\partial t} + \frac{\partial \bar{U}_i k}{\partial x_i} = v_t S^2 - \epsilon + \frac{\partial}{\partial x_j} \left[ \left( v + \frac{v_t}{\sigma_k} \right) \frac{\partial k}{\partial x_j} \right] \quad (4)$$

Dissipation rate:

$$\begin{aligned} \frac{\partial \epsilon}{\partial t} + \frac{\partial \bar{U}_i \epsilon}{\partial x_i} = & C_{\epsilon 1} \frac{\epsilon}{k} v_t S^2 - C_{\epsilon 2} \frac{\epsilon^2}{k} \\ & + \frac{\partial}{\partial x_j} \left[ \left( v + \frac{v_t}{\sigma_\epsilon} \right) \frac{\partial \epsilon}{\partial x_j} \right] \end{aligned} \quad (5)$$

where  $S$  is the turbulent kinetic energy production,  $C_{\mu}$ ,  $\sigma_k$ ,  $\sigma_\epsilon$ ,  $C_{\epsilon 1}$ ,  $C_{\epsilon 2}$  are model coefficients with their values 0.09, 1, 1.3, 1.44, and 1.92 (Sun, et.al., 2008; Salim, et.al., 2011).

### 2.2 Turbine Performance Formulations

After getting the torque value from CFD result, then the coefficient of turbine performance ( $C_p$ ) can be define using the formula:

$$C_p = \frac{\text{Turbine Power}}{\text{Power Potential}} \quad (6)$$

The turbine power ( $P_n$ ) and the power potential ( $P_t$ ) can be define using the formula:

$$P_n = \omega \tau \quad (7)$$

$$P_t = 0.5 \rho A U^3 \quad (8)$$

The torque value ( $\tau$ ) is the result of the numerical modeling while  $\omega$  is initial condition input. The relationship between rotational speed ( $\omega$ ), tip speed ratio (TSR) and current speed ( $U$ ) can be expressed as:

$$TSR = \frac{\omega r}{U} \quad (9)$$

## 3 TURBINE EXPERIMENTAL DATA

Experimenting of the Darrieus turbine with hydrofoil NACA 63 (4) 021 has been carried out in towing tank of Hydrodynamics Laboratory at the University of British Columbia by G.W. Rawlings (2008). The mechanism of the experiment is the Darrieus turbine towed by carriage and combined with the rotation of the electric motor connected by the gearbox to set the turbine rotation during testing.

### 3.1 Turbine Dimension and Characteristic

The turbine has diameter of 0.91 m, consists of 3 blades hydrofoil NACA 63(4)021 with chord 0.07 m and span 0.7 m. The turbine geometry and specifications can be seen in more detail in figure 1 and table 1.

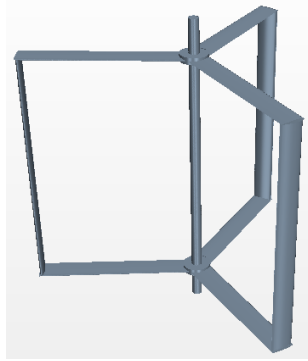


Figure 1: Darrieus turbine geometry (Rawlings, 2008).

Table 1: Principal model turbine parameters (Rawlings, 2008).

Parameter	Dimension and characteristic
Diamater turbine	0.91 m
Number of blades	3
Blade span	0.7 m
Blade profile	NACA 63(4)021
Chord length	0.07 m
Shaft diameter	0.05 m

The turbine geometry in figure 1 can be shown in the 2D sketch (top view) as shown in figure 2.

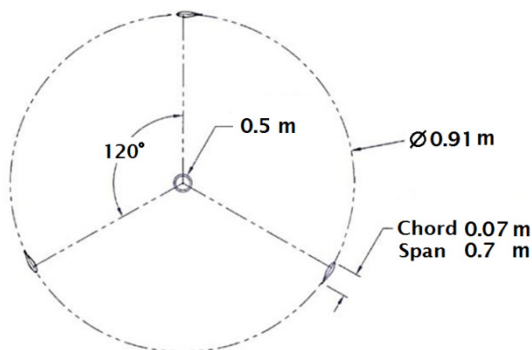


Figure 2: Turbine rotor sketch on top view (Rawlings, 2008).

### 3.2 Turbine Experimental Result

The turbine experimental data is reprocessed based on the turbine performance graph. The experimental

result is processed using the turbine performance formulations, as shown in point 2.2. Turbine experime data can be seen in table 2.

Table 2: Turbine experimental result (Rawlings, 2008; reprocessed).

$U$ (m/s)	TSR	$\omega$ (rad/s)	$\tau$ (N.m)	$P_n$ (watt)	$C_p$
1.5	1.5	4.92	15.32	75.39	0.071
1.5	2.0	6.56	22.46	147.38	0.140
1.5	2.25	7.38	28.93	213.56	0.202
1.5	2.5	8.20	34.12	279.86	0.265
1.5	2.75	9.02	35.73	322.37	0.305
1.5	3.0	9.84	32.57	320.57	0.304
1.5	3.5	11.48	26.12	299.93	0.284

## 4 METHODOLOGY

The numerical simulation begins with creating turbine geometry in .iges format. Next, the turbine geometry is imported into the CFD program and then creates boundary condition geometry and region determination as domain modeling. For the next step, generate grid meshing and do some simulation settings such as selecting solver and input initial condition and then running the simulation.

For validating the numerical modeling output with the experimental result, firstly is to define the boundary geometry dimension, and then study grid meshing independency and compare the turbulence model. The simulation is carried out with varying TSR rate at constant current speed, 1.5 m/s.

Simulation result error is calculated using the formulation:

$$\% \text{ error} = \frac{| \text{experiment} - \text{CFD} |}{\text{experiment}} \times 100 \quad (10)$$

To get the results of numerical modeling at a certain degree of turbine rotation, the time step calculation is required. Meanwhile, to determine a total time for every single simulation, the physical time calculation is required.

The time step in this study was calculated for every 5° turbine revolute. While the physical time is determined 10 times of the turbine rotation at the current speed of 1.5 m/s.

Following is the example of calculating physical time and time step at the turbine rotational speed of 4.92 rad/s.

Physical Time (for 10 times of turbine rotation) can be calculated with the formulation:

$$\omega = \frac{\theta - \theta_0}{\text{Physical Time}} \quad (11)$$

where :

$\theta$  = degree for 1 rotation =  $2\pi$  rad

$\theta_0$  = degree for 0 rotation = 0

So that

$$\begin{aligned} \text{Physical Time} &= \frac{(2\pi - 0)\text{rad}}{4.92 \text{ rad/s}} \times 10 \\ &= 12.8 \text{ s} \end{aligned}$$

Time Step (for every  $5^\circ$  turbine revolute) can be calculated with the formulation:

$$\begin{aligned} \text{Time Step} &= \frac{\text{time for 1 simulation}}{\text{number of steps}} \quad (12) \\ &= \frac{1.28 \text{ s}}{\left(\frac{360^\circ}{5^\circ}\right)} \\ &= 0.018 \text{ s} \end{aligned}$$

The setting of the boundary condition domain in every numerical simulation can be seen in table 3.

Table 3: Boundary condition domain in the numerical modeling simulation.

Region	Boundary condition
Inlet	Uniform flow : 1.5 m/s
Outlet	Pressure : 0 Pa
Side Walls	Slip walls
Top	Symmetry wall
Bottom	Symmetry wall
Turbine	Wall : no slip

## 5 RESULT AND DISCUSSION

### 5.1 Defining Boundary Geometry Dimension

Numerical modeling uses 2D models so that the determination of boundary sizes is sufficient to be analyzed on the dimensions of length and width. Simulation of defining boundary dimensions using the same grid meshing composition, with input current speed of 1.5 m/s and TSR 3.5.

The numerical simulation results based on variations in boundary size can be seen in table 4 and table 5.

Table 4: Determination of boundary length.

Length variations	$\omega$ (rad/s)	$C_p$ (experiment)	$C_p$ (CFD)	Error
L 12D	11.48	0.284	0.286	0.8%
L 14D	11.48	0.284	0.293	2.3%
L 16D	11.48	0.284	0.285	0.4%
L 18D	11.48	0.284	0.287	1.01%

Table 5: Determination of boundary width.

Width variations	$\omega$ (rad/s)	$C_p$ (experiment)	$C_p$ (CFD)	Error
W 4D	11.48	0.284	0.45	59.3%
W 6D	11.48	0.284	0.34	19.4%
W 8D	11.48	0.284	0.29	0.4%
W 10D	11.48	0.284	0.28	2.8%

Based on the simulation results in table 4 and table 5, the dimension of boundary condition geometry is taken 12D in length and 8D in width, where D is the turbine diameter.

### 5.2 Grid Independence Analysis

The independence grid study is conducted to define the best grid composition for getting the best analyzing results. There are several considerations on the meshing process including the number of grids generated, time for meshing, time for simulating, the computer performance and the error value.

In the analysis of grid independence, the simulations are carried out with variation number of grid. Figure 3 shows grid meshing comparison between tenuous and precision density. For the next, to find out the numerical results based on the number of grid density, this study simulates Darrieus turbine on the current velocity of 1.5 m/s and TSR 3.0. The simulation results are presented in table 6.

The simulation result in table 6 shows that the numerical model with the smallest error value is produced when using meshing 5. However, consideration to the computer performance which difficult to generate meshing 9,207,251 cells and need longer time for simulation, so that it is decided to use meshing 4 with error value 3.3%. This error value is not much different from the error value of meshing 5. Moreover, meshing 4 only consists of 73,397 cells after being converted into the 2D model.

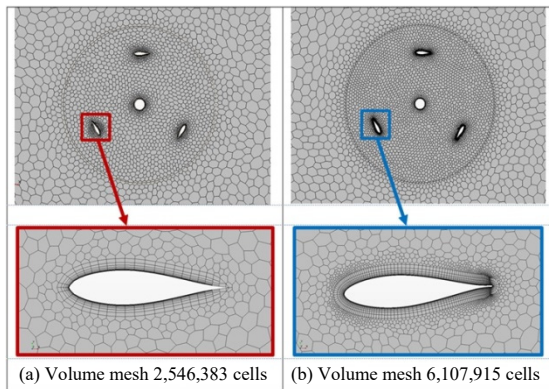


Figure 3: Comparison of meshing results when using tenuuous grid (a) and precision grid (b).

Table 6: Numerical simulation results based on number grids variations.

Meshing variations	Grids number		Time for simulation (minutes)	Error
	Model 3D	Covert to 2D		
Meshing 1	1,387,775	66,410	38	20.4%
Meshing 2	2,546,383	68,619	45	18.5%
Meshing 3	3,944,757	71,394	75	15.2%
Meshing 4	6,107,915	73,397	96	3.3%
Meshing 5	9,207,251	78,295	135	0.8%

### 5.3 Turbulence Model Comparison

One of the factors that have a great effect on the result of the CFD analysis is the flow turbulence model. The numerical validation process in this study simulates several turbulence models to define what turbulence model produces the smallest error values. The turbulence models that compared in this study are  $k-\epsilon$ ,  $k-\omega$  SST, Spalart Allmaras and Reynolds Stress Turbulence.

Turbulence model comparison is performed at the current velocity of 1.5 m/s, TSR 2.5, and using the turbulence intensity of 0.05 (Marsh, 2015,2016). The simulation result of the turbulence model comparison can be seen in table 7.

The simulation result in table 7 shows that the smallest error is produced by  $k-\omega$  SST turbulence model. This result has corresponded with many studies (Dai, 2009; Marsh, 2015; 2016; Castelli, 2010; Rahmawati, 2017; Nobile, 2011; Madi, et.al., 2019) who used the  $k-\omega$  SST model in their ocean current turbine numerical model.

Table 7: The result of turbulence model comparison.

Turbulence Models	$\tau$ (experiment) (N.m)	$\tau$ (CFD) (N.m)	Error
$k-\epsilon$	34.12	38.11	11.7%
$k-\omega$ SST	34.12	36.67	7.5%
Spalart Allmaras	34.12	39.42	15.5%
Reynolds Stress Turbulence	34.12	26.62	22%

### 5.4 Numerical Validation Result

After defining boundary geometry dimensions, grid independency analysis, and selecting the turbulence model appropriate, then the next step is validation the numerical model of Darrieus turbine with the experimental result. The validation parameter is the torque that correlates with the performance coefficient.

#### 5.4.1 Torque Validation

Torque simulation for the validation process is performed at the current speed of 2 m/s and TSR 2.5. The result of torque using numerical model CFD is shown in figure 4 and validation with the experimental result is shown in figure 5.

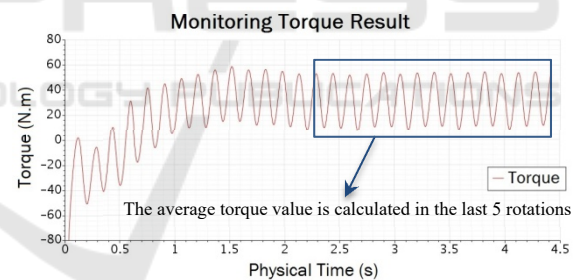


Figure 4: Torque result of numerical modeling at the current speed of 2 m/s and TSR 2.5.

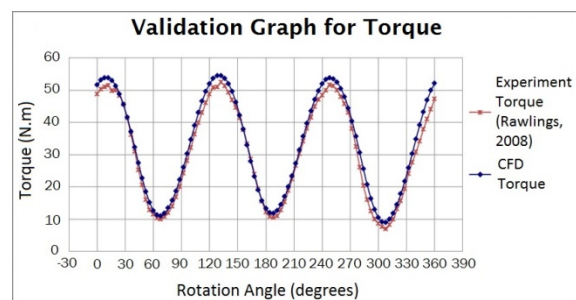


Figure 5: Torque validation at the current speed of 2 m/s and TSR 2.5 for 1 rotation.



One of the torque validation can be seen in figure 5. On the figure, both experimental torque and CFD torque are simulated at the current speed of 2 m/s and TSR 2.5. The validation torque on this condition has error value of 7.02%.

### 5.4.2 Coefficient of Performance (Cp) Validation

The coefficient of performance well known as turbine efficiency is the ratio between power produced by the turbine operating with the potential current energy absorbed by the turbine theoretically. Turbine efficiency and its validation can be calculated using several data such as turbine dimension, current velocity and torque result both from experimental testing and CFD analysis.

For example, turbine efficiency and its validation are calculated at the current speed of 1.5 m/s, TSR 1.5.

Using equation 8, the theoretical power potential of the turbine can be calculated

$$P_t = 0.5 \times 1000 \text{ kg/m}^3 \times (0.91 \text{ m} \times 0.7 \text{ m}) \times (1.5 \text{ m/s})^3 = 1055.64 \text{ watt}$$

Using equation 7, the turbine power from CFD analysis can be calculated.

$$P_{nCFD} = 4.92 \text{ rad/s} \times 16.59 \text{ N.m} = 81.65 \text{ watt}$$

The result of turbine efficiency from CFD analysis can be calculated using equation 6.

$$C_{pCFD} = 81.65 \text{ watt} / 1055.64 \text{ watt} = 0.077$$

By using the experimental data in table 2, the validation of turbine efficiency can be calculated using equation 10.

$$\% \text{ error} = ([0.071 - 0.077] / 0.07) \times 100 = 8.3 \%$$

The validation results of CFD analysis and experimental data of turbine Darrieus can be seen in detail in table 8 and figure 6.

Table 8 shows the comparison between the CFD analysis and the experimental results. CFD analysis uses initial conditions which are equated with

Table 8: The validation of Darrieus turbine numerical CFD and experimental results.

U m/s	TSR	ω (rad/s)	Pt (watt)	Experimental result (Rawlings, 2008; reprocessed)			Numerical CFD			Error
				τ (N.m)	Pn (watt)	Cp	τ (N.m)	Pn (watt)	Cp	
1.5	1.5	4.92	1055.64	15.32	75.39	0.071	16.59	81.65	0.077	8.3%
1.5	2.0	6.56	1055.64	22.46	147.38	0.140	26.17	171.70	0.163	16.5%
1.5	2.25	7.38	1055.64	28.93	213.56	0.202	31.73	234.21	0.222	9.7%
1.5	2.5	8.20	1055.64	34.12	279.86	0.265	36.67	300.77	0.285	7.5%
1.5	2.75	9.02	1055.64	35.73	322.37	0.305	37.64	339.62	0.322	5.4%
1.5	3.0	9.84	1055.64	32.57	320.57	0.304	33.63	330.98	0.314	3.3%
1.5	3.5	11.48	1055.64	26.12	299.93	0.284	26.23	301.23	0.285	0.4%

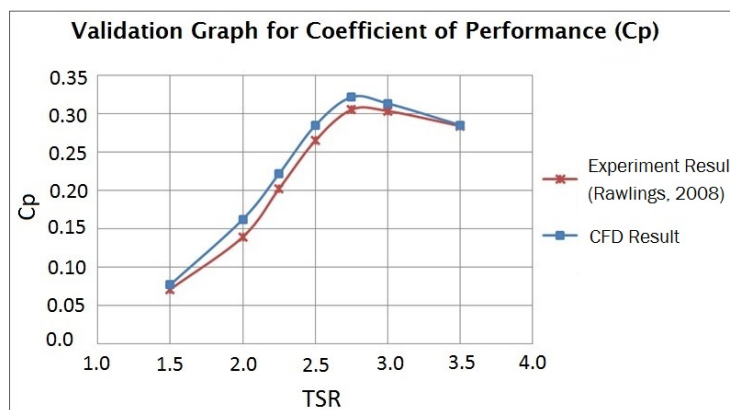


Figure 6: Darrieus turbine performance on numerical CFD and experimental results.

experimental data that are simulated at the current speed of 1.5 m/s with TSR variations between 1.5 to 3.5. Validation results are obtained numerical model error value at TSR 1.5 is 8.3%, TSR 2.0 is 16.5%, TSR 2.25 is 9.7%, TSR 2.5 is 7.5%, TSR 2.75 is 5.4%, TSR 3.0 is 3.3%, and at TSR 3.5 is 0.4%.

Figure 6 shows that the  $C_p$  of the CFD analysis results tend to be higher than the  $C_p$  of the experimental results because numerical analysis uses 2D models that ignore the influence of the turbine arm in the simulation. Basically the turbine arm will produce a drag force which can reduce turbine performance.

The numerical modeling results of the Darrieus turbine are presented in the flow direction vector that trough pass the turbine and flow velocity contour as shown in figures 7 and 8. In these figures, the Darrieus turbine is simulated at the free stream speed of 1.5 m/s with TSR 2.75 (figure 7) and TSR 3.5 (figure 8).

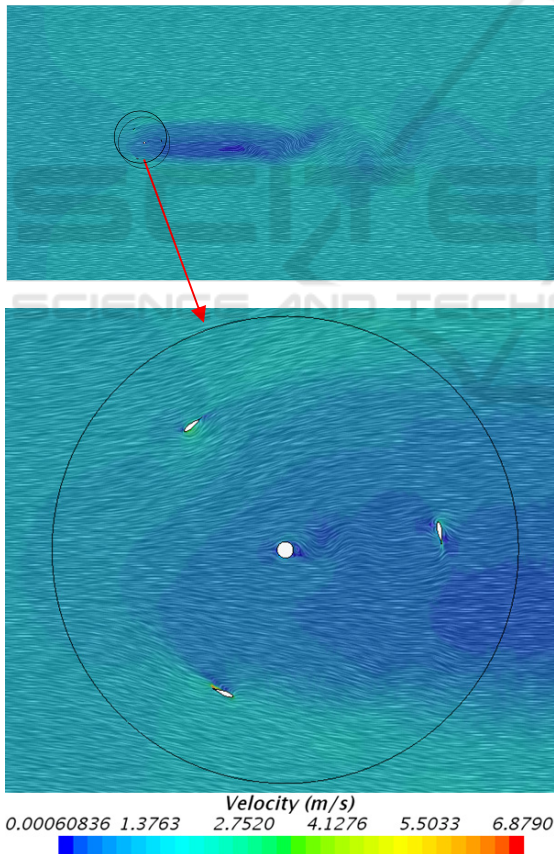


Figure 7: Flow velocity direction on the turbine, rotating at TSR 2.75.

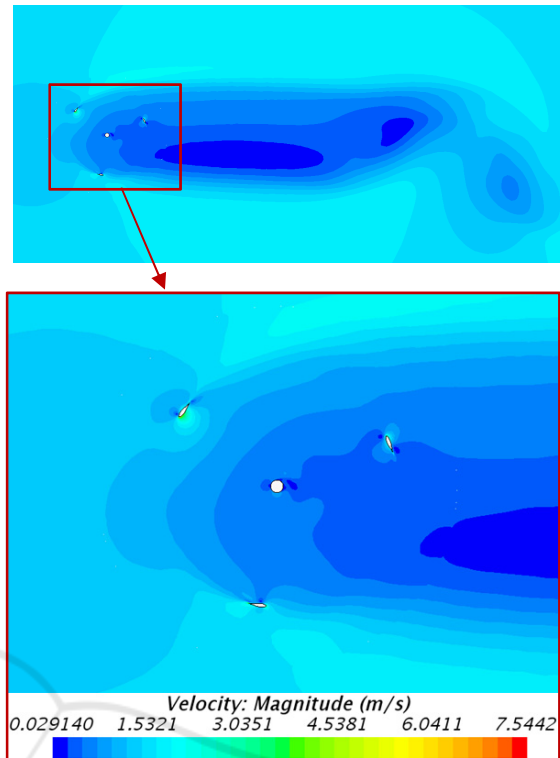


Figure 8: Flow velocity contour on the turbine, rotating at TSR 3.5.

## 6 CONCLUSION

Validation of the Darrieus turbine numerical model starts from defining the boundary geometry dimension, study the grid independency, and selecting the turbulence model appropriate. The numerical modeling error value at TSR 1.5 is 8.3%, TSR 2.0 is 16.5%, TSR 2.25 is 9.7%, TSR 2.5 is 7.5%, TSR 2.75 is 5.4%, TSR 3.0 is 3.3%, and at TSR 3.5 is 0.4%. The average error is 7.3% which is categorized as a good agreement result.

## ACKNOWLEDGMENTS

A great appreciation to supervisors and all members of Marine Engineering Postgraduate Laboratorium, Sepuluh Nopember Institut of Technology Surabaya for support throughout the project. Authors also would like to thanks all colleagues from Agency for the Assessment and Application of Technology (BPPT) especially the work unit of Center of Technology for Maritime Industrial (PTRIM) and

Hydrodynamic Institute of Technology (BTH) for providing facility and supporting the project.

## REFERENCES

- Castelli, M. R., Ardizzon, G., Battisti, L., Benini, E., Pavesi, G., 2010. Modeling Strategy and Numerical Validation for a Darrieus Vertical Axis Micro-wind Turbine. In *International Mechanical Engineering Congress and Exposition*. ASME.
- Dai, Y. M., Lam, W., 2009. Numerical Study of Straight-bladed Darrieus-type Tidal Turbine. In *ICE-Energy*; 162:67-76.
- Daruwedho, H., Sasmito, B., Janu, A. F., 2016. Analysis of Sea Surface Levels in Indonesian Waters Using the Jason-2 Altimetry Satellite 2010-2014 (in Indonesian language). In *Jurnal Geodesi Undip*; 5(2):145-158.
- Hantoro, R., Prananda, J., Mahmashani, A. W., Septyaningru, E., and Imanuddin, E., 2018. Performance Investigation of an Innovative Vertical Axis Hydrokinetic Turbine-Straight Blade Cascaded (VAHT-SBC) for Low Current Speed. In *Journal of Physics*; 1022: 1-8. IOP Publishing.
- Hantoro, R., Utama, I. K. A. P., Erwandi, Sulisetyono, A., 2009. Force Instability and Fluid-Structure Interaction in Vertical Axis Turbines for Generating Tidal Current Energy (in Indonesian language). In *Jurnal Teknik Mesin*; 11(1):25-33.
- Hantoro, R., Utama, I. K. A. P., Erwandi, Sulisetyono, A., 2011. An Experimental Investigation of Passive Variable-Pitch Vertical-Axis Ocean Current Turbine. In *ITB J Eng Sci*; 43(1):27-40.
- Kasharjanto, A., Rahuna, D., Aditya, R. B., 2017. Test Performance of Tidal Current Turbine 10 Kilowatt using Double Hull Platform on the Suramadu Bridge (in Indonesian language). In *Jurnal Ilmu Pengetahuan & Teknologi Kelautan*; 14:79-86.
- Madi, Sasono, M. E. N., Hadiwidodo, Y. S., Sujiatanti, S. H., 2019. Application of Savonius Turbine behind The Propeller as Energy Source of Fishing Vessel in Indonesia. In *IOP Conference Series: Materials Science and Engineering*. IOP Publishing.
- Marsh, P., Ranmuthugala, D., Penesis, I., Thomas, G., 2015. Numerical Investigation of the Influence of Blade Helicity on the Performance Characteristics of Vertical Axis Tidal Turbines. In *Renewable Energy*; 81:926-935. ELSEVIER.
- Marsh, P., Ranmuthugala, D., Penesis, I., Thomas, G., 2015. Three-Dimensional Numerical Simulations of Straight-bladed Vertical Axis Tidal Turbines Investigating Power Output, Torque Ripple and Mounting Forces. In *Renewable Energy*; 81:67-77. ELSEVIER.
- Marsh, P., Ranmuthugala, D., Penesis, I., Thomas, G., 2016. Numerical Simulation of the Loading Characteristics of Straight and Helical-bladed Vertical Axis Tidal Turbines. In *Renewable Energy*; 94:418-428. ELSEVIER.
- MeyGen, 2019. SSIMEC Atlantis Energy. In <https://simecatlantis.com/projects/meygen>. (accessed on 17 October 2019).
- Mukhtasor, Susilohadi, Erwandi, Pandoe, W., Iswadi, A., Firdaus, A. M., Prabowo, H., Sudjono, E., Prasetyo, E., and Ilahude, D., 2014. *Ocean Energy Resources in Indonesia (in Indonesian language)*. Marine Geological Research and Development Center (P3GL) Ministry of Energy and Mineral Resources, Association of Marine Energy of Indonesia (ASELI).
- Muluaem, 2012. *Simplified CFD Modelling of Tidal Turbines for Exploring Arrays of Devices*. Thesis PhD. University of Exeter.
- Nobile, R., Vahdati, M., Barlow, J. F., Mewburn-Crook, A., 2011. Dynamic Stall for a Vertical Axis Wind Turbine in a Two-Dimensional Study. In *World Renewable Energy Congress: 4225-4232*. LINKÖPINGS UNIVERSITET.
- Rachmat, B., and Ilahude, D., 2015. Determining Location of Tidal Current Turbine Power Plant-Small Scale in Liatung Starit, Talaud, North Sulawesi (in Indonesian language). In *Jurnal Geologi Kelautan*; 13(3):127-142.
- Rahmawati, S., 2017. *Study on Characteristics of Tidal Current Energy and Ocean Environmental Pollution at Indonesia Archipelago*. Doctor Dissertation. Hiroshima University.
- Rawlings, G. W., 2008. *Parametric Characterization of an Experimental Vertical Axis Hydro Turbine*, Thesis, Faculty of Graduate Studies (Mechanical Engineering): University of British Columbia, Vancouver.
- Salim, M., Buccolieri, R., Chan, A., Sabatino, S., 2011. Numerical Simulation of Atmospheric Pollutant Dispersion in an Urban Street Canyon: Comparison Between RANS and LES. In *Journal of Wind Engineering and Industrial Aerodynamics*; 99(2):103-113. ELSEVIER.
- Sun, X., Chick, J., Bryden, G., 2008. Laboratory-scale Simulation of Energy Extraction From Tidal Currents. In *Renewable Energy*; 33(6):1267-1274. ELSEVIER.